International Journal of Scientific Research in Science and Technology
Print ISSN: 2395-6011 | Online ISSN: 2395-602X (www.ijsrst.com)
© 2021 | IJSRST | Volume 8 - Issue 1

Study of Morphological and Dielectrical Properties of Zr-Co Doped Barium Hexaferrite

D.J.Roy[1*], A.R.Bansod[2], K.G.Rewatkar[2], N.S.Kokode[3]

[1]AbhaGaikwad- Patil College of Engg., Nagpur, Maharashtra, India

[2]Dr. Ambedkar College Dikshabhoomi, Nagpur, Maharashtra, India

[3]N.H.College, Bramhapuri, Chandrapur, Maharashtra, India

ABSTRACT

A sequence of hexaferrite specimen with a molecular formula $BaFe_{12-2x}Co_xZr_xO_{19}$ were synthesised using a traditional Microwave assisted Sol-gel auto-combustion process, where ferrites powder were processed by continual heat in the form of radiation through microwave. All the required nitrates were taken in stoichemetric proportion along with Urea, which provide requisite energy during the exothermic reaction in order to form ferrites materials powder. Microwave used in these method provide uniform heating leads to the ultrafast morphological transformation which results into nano-sized ferrites powder obtained. The structural and morphological properties studied by using X-ray diffractometer and Scanning Electron Microscope which reveals the prevalent hexagonal structure of space group symmetry $P6_3/mmc$. The dielectric features of the ferrites powder were studied at a frequency ranging from 100 Hz to 1 MHz at room temperature. The dielectric observation of synthesized hexaferrites reveals a drop in dielectric constants and a rise in dielectric loss with an increase in Co-Zr substitutions.

Keywords : XRD; SEM, Dielectric Properties, Ba- hexaferrites

I. INTRODUCTION

Substances possessing substantial dielectric and magnetic assets at the same time seem to be of considerable interest to contemporary science from the point of view with their ability for technical implementations to electrical equipment and structures. The sudden growth of elevated speed wireless communications involves the advancement of efficient, portable,and affordable technologies which could be utilized across a large frequency band [1-4]. Dielectric materials carry a vital character in international community of an extensive variety of implementations ranging through conventional to satellite telecommunications, which include radio, GPS and DBS Television. Microwave devices relying upon substances containing enhanced dielectric features are needed to meet the needs of existing as well as futuristic technologies. Hexaferrites are a large class one of ferrite materials attributable towards various uses throughout audio media, filters, oscilloscopes and antennas within that telecommunication sector[5, 6].A further benefit being there chemical consistency enables themselves

as environment-friendly and effective. The electrical and magnetic characteristics of barium hexaferrites ($BaFe_{12}O_{19}$) has been modified by composition variation, that results into morphological alteration of barium hexaferrites by orientation and positioning of the inclusion ions. Hexa-ferrites show the phenomena of universal ferromagnetic resonance which may be used successfully even an absence of applied magnetic field and often used in communications and military purposes [5, 7, 8]. A substantial amount of research being executed in the domain of hexaferrites within a past decade, wherein coupled replacements has been made in spite of Fe ions [9,10] or altered the methodology of formulation[11,12]. In this research module, trivalent Fe ions in barium hexaferrites are replaced by a group of divalent Cobalt (Co^{2+}) and tetravalent Zirconium (Zr^{4+}) ions in various concentrations. In addition, hexaferrites have been of concern for not only their magnetic behaviour, but also because of their dielectric polarisation found in their composition [14].

II. EXPERIMENTAL

Numbers of technique is available to synthesize ferrites materials such as co-precipitation method, glass crystallization, hydrothermal method of synthesis, solid state reaction, [6]etc. Out of which we use simple and efficient Sol-gel Induced auto-combustion method for synthesis of required hexaferrites due to its simplicity in processing, low annealing temperature, and very short reaction time. In addition the Sol-gel auto-combustion method produces ultra-fine nano materials with a substantial circulation of particle sizes, outstanding chemical uniformity and the probability of creating a unified single domain structure.

Hexaferrite powders with compounds with chemical formula $BaFe_{12-2x}(CoZr)_xO_{19}$ (with x = 0.0, 0.2, 0.4, 0.6, 1.0) were synthesized by Microwave Induce sol-gel auto combustion technique in which microwave provides an uniform radiation in the form of heat to the specimen within the process of combustions. AR grade Nitrates such as $Ba(NO_3)_2$, $Co(NO_3)_2$, $ZrO(NO_3)_2$ and $Fe(NO_3)_3$ with urea are taken in stoichiometric proportion then dissolve into unionized double filtered distilled water at temperature of about 70^0C for 20-25 minutes. Urea supply sufficient amount of energy to start an exothermic reaction. Converted gel placed a side for an hour at room temperature. And then gel is placed within digitally controlled microwave of 2.5 GHz for 15 minutes, The gel get burnt and finally converted into ferrites powders. As obtained ferrites powder are grinded for 4 hour then housed in a muffle furnace for sintering at about 800^0C for 4 hours with gradually slow cooling at rate of 50^0C/minute along with further grinding of few hours.

XRD and SEM were utilized to analyzed the Structural and morphological properties of fabricated ferrites materials. A comprehensive study on the dielectric nature and electricalconductivity of $BaFe_{12-2x}(CoZr)_xO_{19}$has been undertaken within the frequency band from 10 kHz to 1MHz employing Wayne Kerr-WK6500B Impedance Analyzer.

III. RESULTS AND DISCUSSION

X-ray Diffraction (XRD) Analysis:

The X-ray diffractograph of BaFe(12-2x)(CoZr) xO19hexaferrites (x=0.0,0.2,0.4,0.6,and 1.0) specimens within analysis have been collected by using Philips X'pertDiffractometerutilising Cu-Kα radiation of wavelength $\lambda = 1.542$ Å which are shown in Fig.1, consisting reference peaks of M-type Barium nanoferrites relating to space group symmetry P63/mmc alluded fromthe standard JCPDS index. From the most intense peaks, the values of Miller indices (h k l) correlating to the inter-planer

distance d(hkl)are employing to determine the values of lattice constants 'a' and'c' according to the equation

$$\frac{1}{d_{hkl}^2} = \frac{4}{3}\left[\frac{h^2+hk+k^2}{a^2}\right] + \frac{l^2}{c^2}$$

The unit cell volume can beobtained by using formula

$$V = 0.866a2c$$

The X- ray density Dxoftendeterminedusing the equation

$$Dx = \frac{zM}{VN_A}$$

In which z represent the number of molecules in a unit cell and equal to 2 for hexaferrites, M is themolecular weight of sample, N_A is Avogadro's number.From the **Table 1**, the values of c/a are below the value 3.98 for all synthesized materials give the confirmation of formation of BaMhexaferrites. The unit cell volume (V) continues to increase as replacement level grows, owing to the greater radii of the replaced Zr^{4+}(0.72A°) and Co^{2+}(0.70A°) ions than the Fe^{3+}(0.64A°) showed in **Figure 2**.The value of lattice parameter 'c' rises from 23.1619 to 23.1972 A° for doping concentration x = 0.0 to x = 1.0, that suggests unit cell enhancement throughthe c-axis that is attributed to the increased gapwithin the Fe^{3+}- O^{2-} ions as well as the decreased super-exchange interactions of $Fe^{3+} \leftrightarrow Fe^{2+}$.

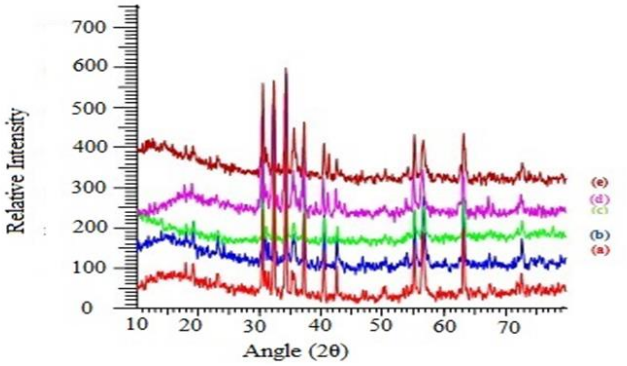

Figure 1: XRD images for $Ba(Co\text{-}Zr)_xFe_{12-2x}O_{19}$(x =0.0(a),0.2(b),0.4(c),0.6(d), 1(e))

Table 1: Structural parameters such as lattice parameters (a, c,), c/a ratio, Unit cell volume (V), densities ($\rho_{x\text{-}ray}$, ρ_m), and porosity (P).

Conc. (x)	Lattice parameters (Å)		$\frac{c}{a}$	Volume (Å^3)	Density x-ray ($\rho_{x\text{-}ray}$) (gm/cm^3)	Density Mass (ρ_m) (gm/cm^3)	Porosity (%)
	a	c					
0.0	5.8835	23.1619	3.93	694.32	5.32	2.607	50.99
0.2	5.8846	23.1940	3.93	694.64	5.35	2.655	50.37
0.4	5.8920	23.1943	3.93	697.30	5.36	2.701	49.60
0.6	5.8835	23.1942	3.94	695.29	5.42	2.741	49.42
1.0	5.8801	23.1972	3.94	695.30	5.49	2.826	48.52

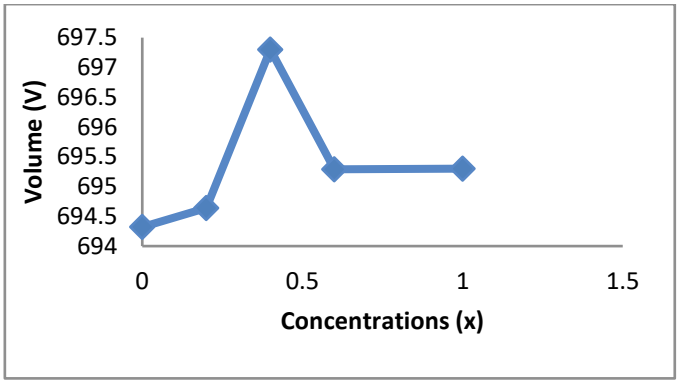

Figure 2: Unit cell volumes for different doping Concentrations (x)

Scanning Electron Microscope (SEM):

Themorphological characterization of thefabricated ferrites materialswas done by utilizing SEM (Model7600F)IIT Bombay[18]and isdepictedin **Figure 3**. The SEM micrograph demonstrates the development nanohexaferrites specimens have approximate grain sizes in between 35 and 50 nm. The photos reveal that the crystallites aren't packaged tightly during the whole sample, highlighting the porous nature of the specimens.It can be shown from the SEM images that the porosity is decreasing as the

volume of doping increases. This outcome complies with the measured porosity values in **Table 1**.

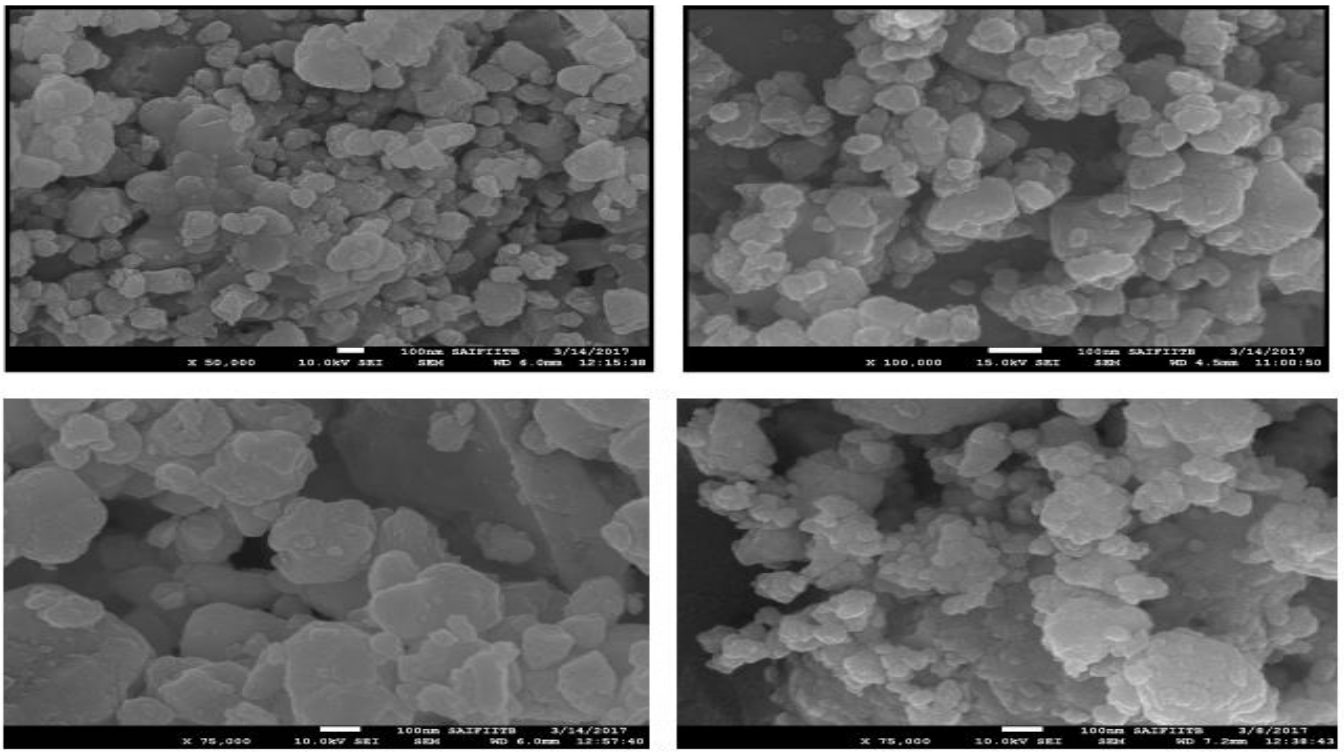

Figure 3: SEM micrograph of $Ba(Co\text{-}Zr)_xFe_{12-2x}O_{19}$,(x=0, 0.4, 0.6, 1)

Electrical Conductivity:

With the help of Wanyekerr Impedance Analyzer data sheet, Electrical Conductivity have been calculated by using simple equation

$$\sigma_{ac}=\frac{Gt}{A}$$

G- represents conductance, A- represents cross sectional area, and t-represents thickness of material pellets [5].

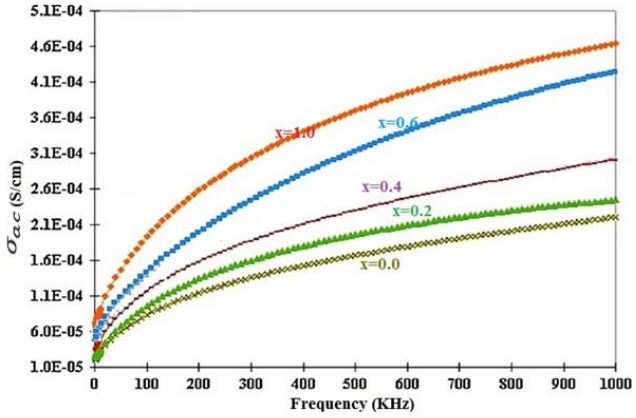

Figure 4: Ac Conductivity of $Ba(CoZr)_xFe_{12-2x}O_{19}$ at different Concentrations and at frequency(KHz)

It's evident from Figure 4, that an electrical conductivity (σ_{ac})goes on increases with the frequency of an external field, which may be interpreted according toVerwey's hopping mechanism, which implies that the conductivity in the ferrites is partly attributable to the hopping of electrons amongst ions of the identical element found in more than one valence state, arbitrarily spread over crystallographically similar lattice sites.Ferrites contain structurally cubic-closed, packed oxygen lattices containing cations at the octahedral (B) and tetrahedral (A) sites. The separation between the two metal (Fe) ions at the B site is less than the difference between a metal ion at the B site and another metal ion at the A site. Thus the probability of the electron hopping between B and A sites is very lesscompare to that of B–B hopping. Andhopping among A-A sites doesn't occur as there are only Fe^{3+} ions at A sites and

any Fe^{2+} ions produced throughout manufacturing ideally settled only on B sites[19, 20].Under the impact of the applied field the charges will transfer, resulting in the electrical behaviour of the specimens. If the applied signal frequency increases, electron hopping increases, leads to an increase in AC conductivity [21, 22]. Electrical conductivity declinesby increase in the concentration of Zr^{4+}-Co^{2+} ions. The porosity of the specimen decreases with an increase in concentrations of substituent's **(Table 1),** because of which the distance amongst the grains increases, leading to an impediment in the conduction within grains.

Dielectric Analysis:

Impedance Analyzer is utilised to study the Dielectric behavioursof specimen materialswithin a frequency ranging from 1 KHz to 1MHz.The dielectric constant(ε') ofthefabricated materialis obtained by

$$\varepsilon' = Ct/A\varepsilon_0$$

ε_0 - represents permittivity of free space = 8.85 x 10^{-12}F/m, C- represents capacitance of the specimen, t - represents thickness of the specimen pellets, and A - represents cross-sectional area of the specimen pellets [4].

The dielectric tangent loss is again measure using the equation

$$\tan\delta = \varepsilon''/\varepsilon'$$

wheretanδ is dielectric loss.

The response of dielectric constant (ε') of formulated ferrites materialsto the frequency and doping concentrationsis presented in **Figure 5.**

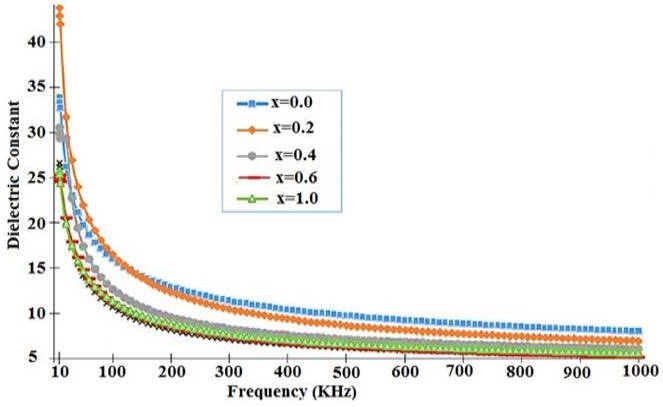

Figure 5:Frequency dependent Dielectric Constant for $Ba(CoZr)_xFe_{12-2x}O_{19}$.

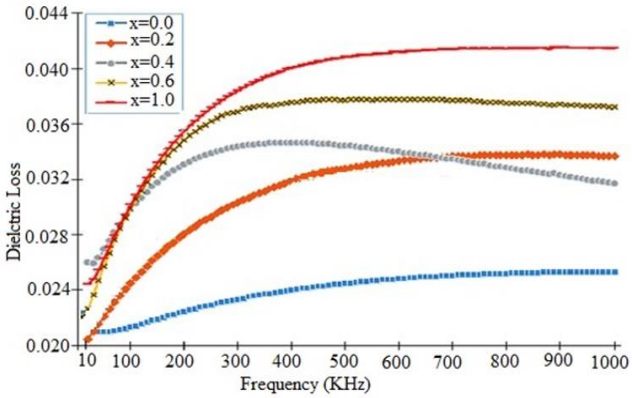

Figure 6: Variation of Dielectric losses for $Ba(CoZr)_xFe_{12-2x}O19$ with Frequency at different concentration.

Figure 5 displays the dielectric constant (ε') for all synthesised ferrites materials are frequency dependant. With increase in the frequency of an applied field, the dielectric constant (ε') reduces. At the lower frequency the dielectric constant is maximum, and that is reduces with increase in frequency owing to dielectric relaxation and dielectric dispersion, that Koop's theory can clarify. In Accordance to Koop's theory, the dielectric system is comprised of two layers, one is conducting grains and the next one is of non-conducting grain boundaries. The charged particles in the substance require a definite time to line up in the direction of applied field, and this time is preferred asrelaxation time. If the frequency of applied field is raisebeyonda defined limit, then the material ions unable to line upalongside the field direction in such a way that the polarisation unable toachieve at its saturation sothere is decrease in Dielectric Constant [23, 24].With the increased Zr-Co ions, ferric ions are decreased inB-sites. Fe^{3+} ions were essentially accountable for the polarisation of space charges as well asfor the hopping mechanism within localised state. Consequently, a rise in the content of Zr-Co ions induces a decrease in polarisation and hopping amongst theFe^{3+} and Fe^{2+} that cause lowering the value of ε' of formulated samples being examined. The higher values

of ε' obtained withdoping were favourable forimpedance matching.It is obvious from**Figure 6,** the loss tangent rise by up to 500 kHz and later it become nearly constant for all samples. The key element that governs dielectric losses is the hopping of electrons ($Fe^{3+} \leftrightarrow Fe^{2+}$)from octahedral to tetrahedral sites.Initially, the loss parameter increases because of polarisation losses and loss due to electric conductancebesidefrequency [25]. At sufficiently elevated frequency, ions areunable to hopp and thus interfacial polarisation can be reduced [26]. Thus, after 500 kHz, dielectric loss activity is almost constant (Fig. 6).The increasing dielectric losses have also been observed as a result of a raise in the doping concentration which is resulting from the increasing hopping process from octaredral (B) to tetrahedral (A)sites. In addition, the radii of Zr^{4+} and Co^{2+} ions greater as compared to Fe^{3+}, an extra intrinsic electric moment developed. These intrinsic moment rises through rise in doping concentration leading to an increasingDielectric loss[27].The improvement in dielectric loss byreplacement make this ferrites sample compressed, thereby making them ideal for absorption purposes.

IV. CONCLUSION

The Zr^{4+}- Co^{2+} substituted Ba hexaferritesof chemical formula$BaFe_{(12-2x)}Co_xZr_xO_{19}$(x= 0.0 to 1.0) have been processed by Microwave induced Sol-gel auto-combustion route.The XRD investigation of the synthesized nano-particles documented the formulation of mono phase M- type hexagonal ferrites. As the frequency increases, electrical conductivity and loss tangent increases, simultaneously the values of Di-electric constant decreases. But, as the Zr^{4+}-Co^{2+} as doping concentration raises, the value of electrical conductivity and dielectric constant decreases, simultaneously loss tangent increases. The study of suchhexagonal ferritesput forward as an effective choice for applications in microwave such as absorption and Impedance matching.

V. REFERENCES

[1]. R.D.C. Lima, M.S. Pinho, M.L. Gregori, R.C.R. Nunes, T. Ogasawara, Mater. Sci-Poland.2004,22(3), 245–252.

[2]. S.P. Gairola, V. Verma, A. Singh, L.P. Purohit, R.K. Kotnala, Solid State Commun.2010,150(3–4), 147–151.

[3]. M.R. Meshram, N.K. Agrawal, B. Sinha, P.S. Misra, J. Magn. Mater.2004,271(2–3), 207–214.

[4]. U. Ozgur, Y. Alivov, H. Morkoc, J. Mater. Sci. Mater. Electron.2009, 20(9), 789–834.

[5]. A. Singh, S.B. Narang, K. Singh, O.P. Pandey, R.K. Kotnala, J. Ceram. Process. Res.2010,11(2), 241–249.

[6]. F.J. Berry, J.F. Marco, C.B. Ponton, K.R. White, J. Mater. Sci. Mater. Electron.2001,20(5), 431–434.

[7]. S.B. Narang, A. Singh, K. Singh, J. Ceram. Process. Res.2007,8(5), 347–351.

[8]. S. Pignard, H. Vincent, E. Flavin, F. Boust, J. Magn. Magn. Mater.2003, 260, 437–446.

[9]. Y. Chen, X. Ren, J. Mater. Sci. Mater. Electron.2016, 27(1), 772–775.

[10]. 10.Y. Song, J. Zheng, M. Sun, S. Zhao, J. Mater. Sci. Mater. Electron.2016, 27(4), 4131–4138.

[11]. M.M. Rashad, I.A. Ibrahim, J. Mater. Sci. Mater. Electron.2011, 22,1796.

[12]. C.L. Yuan, J. Mater. Sci. Mater. Electron.2016, 27(5), 4908–4912.

[13]. C. Doroftei, E. Rezlescu, P.D. Popa, N. Rezlescu, J. Optoelectron. Adv. Mater.2006, 8(3), 1023–1027.

[14]. R.S. Meena, S. Bhattachrya, R. Chatterjee, J. Magn. Magn. Mater.2010, 322(14), 1923–1928.

[15]. A. Ghasemi, A. Hossienpour, A. Morisako, A. Saatchi, M. Salehi, J. Magn. Magn. Mater.2006,302(2), 429–435.

[16]. A. Ghasemi, A. Hossienpour, A. Morisako, X. Liu, A. Ashrafizadeh, Mater. Design.2008, 29(1), 112–117.
[17]. Y.J. Kim, S.S. Kim, J. Electroceram.2009, 24(4), 314–318.
[18]. C. Singh, S.B. Narang, I.S. Hudiara, K. Sudheendran, K.C.J. Raju, J. Magn. Magn. Mater.2008, 320, 1657–1665.
[19]. E. Pervaiz, I.H. Gul, J. Magn. Magn. Mater.2014, 349, 27–34.
[20]. S.M. El-Sayed, T.M. Meaz, M.A. Amer, H.A. El Shersaby, Phys. B Phys. Condens. Matter.2013, 426, 137–143.
[21]. S. Hussain, A. Maqsood, J. Alloys Compd.2008, 466(1–2), 293–298.